Journal of Nuclear Materials 402 (2010) 173–178

Contents lists available at ScienceDirect

Journal of Nuclear Materials

journal homepage: www.elsevier.com/locate/jnucmat

Mineral phases and properties of alkali-activated metakaolin-slag hydroceramics for a disposal of simulated highly-alkaline wastes

Song Chen *, Mengqiang Wu, Shuren Zhang

School of Microelectronics and Solid State Electronics, University of Electronic Science and Technology of China, Chengdu 610054, People's Republic of China

ARTICLE INFO

Article history:
Received 16 December 2009
Accepted 20 May 2010

ABSTRACT

An alkali-activated metakaolin-slag hydroceramic (AMSHC) were made from a mixture of metakaolin and slag with a pure alkali solution of sodium hydroxide and a simulated high-alkaline waste (SAW) liquid via a hydrothermal curing for 24 h, respectively. The affecting factors including curing temperature, content of slag and dosage of simulated highly-alkaline waste on the properties of AMSHC, such as adsorption capacity, compressive strength and immobilization, were investigated in detail. Results indicated that the properties of AMSHC were relevant to the chemical composition and the curing conditions. Adding slag to AMSHC can enhance the compressive strength of AMSHC, but also reduce immobilization toward Sr and Cs ions. In addition, an elevated temperature is beneficial to enhance the compressive strength and the immobilization properties.

1. Introduction

Immobilization of radioactive waste is one of crucial technologies in nuclear applications. Many materials including glasses, glass composites, ceramics and cement, etc. can be chosen to immobilize radioactive wastes [1,2]. Currently, one of research interests in the alternative materials is to develop radioactive waste form materials with nature analogue minerals. It is believed [2,3] that the nature analogue minerals can availably achieve the stable and long-term geological disposal of radioactive wastes. With the idea, single and multiphase ceramics with nature analogue [4–7] can be applied to immobilization technology. Especially, the fabrication of glass composite materials incorporating various virtues of ceramic and glass shows a development trend of immobilization technology towards reliability and convenience [2,8,9]. Therefore, the fabrication of nature analogue minerals for radioactive waste forms and a exploitation of a convenient immobilization process is of interest and significative to the development of immobilization technology. Recently, a zeolite-like materials, hydroceramic [10–12], is developed to host a highly-alkaline waste, which [1,11,13,14] is a sodium hydroxide rich waste containing short-lived radioactive nuclides (^{137}Cs and ^{90}Sr) and small amount of sodium salts. The hydroceramic containing zeolite mineral phases is relatively easier to synthesize from a wide range of alumino-silicate materials (e.g. metakaolin, ash fly) via an alkali-activated effect and curing under a mild hydrothermal condition. Because the zeolite structures characterized by lattice positions, channels and voids, may sequester cations and salt molecules, hydroceramic is available to solidify highly-alkaline wastes as one of the best alternative materials. Especially, the zeolite-like minerals in hydroceramic is analogous to nature zeolite-like minerals such as zeolite A, sodalite and cancrinite, which can widely and stably exist in nature conditions. The fabrication of a hydroceramic, thus, can well incorporate with the conception of nature analogue. Also, as an alkali-activated processing, a hydroceramic is well suited to the immobilization of the highly-alkaline waste. For a better understanding on the immobilization and mechanical properties of AMSHC, the present work is to investigate the AMSHC matrix's mechanical properties and the adsorption capacity to Sr, Cs ions. In addition, based on the results, we may then determine an available chemical composition for the subsequent research of the immobilization on a simulated high-alkaline waste liquid and the desired mechanical performance. Similarly, correlation between the mineral compositions and the properties of AMSHC will be also discussed in detail.

2. Experimental

2.1. Raw materials

Kaolinite was obtained from Beichuan County in Sichuan Province, China. Metakaolin used in this work was manufactured by calcining the kaolinite at 750 °C for 2 h. A blast-furnace slag was purchased from Chengdu Iron & Steel Co. Ltd., China. All the above raw materials were ground to 0.5–1.0 μm in diameter. The approximate composition of the raw materials is listed in Table 1.

* Corresponding author. Tel.: +86 28 8320 8048.
E-mail address: chensong77520@163.com (S. Chen).

0022-3115/$ - see front matter © 2010 Elsevier B.V. All rights reserved.
doi:10.1016/j.jnucmat.2010.05.015

Table 1
The chemical composition of raw materials (wt.%).

Material	Loss	SiO_2	Al_2O_3	Fe_2O_3	CaO	MgO	Na_2O	TiO_2
Slag	–	32.27	13.38	1.65	40.14	6.36	–	1.98
Kaolinite	11.62	46.15	38.71	0.05	0.49	0.04	0.004	–

Table 2 summarizes the chemical composition of the simulated highly-alkaline waste (SAW) made from a mixture of several sodium slats, nonradioactive strontium and cesium slats in a sodium hydroxide solution.

2.2. Sample synthesis process

The proportion for AMSHC synthesis are listed in Table 3, and every sample is denoted by a format of ASMHCX-*Y*-*Z*, where A is for alkali-activated, M for metakaolin, S for slag; HC for hydroceramic, *X* for dosage of slag; *Y* for dosage of the simulated highly-alkaline waste liquid and *Z* for curing temperature, respectively.

According to the proportions in Table 3, AMSHC samples were made form a mixture of metakaolin and slag with a sodium hydroxide solution and a simulated highly-alkaline waste solution, respectively. The ratio of liquid to solid was regulated to 0.45. Sample pastes were molded in a stainless steel mold with an identical size of 20 mm × 20 mm × 20 mm, and then procured at room temperature until getting hard. After demolding, all samples were put in a sealed Teflon reactor, and cured hydrothermally at 90 °C, 120 °C and 180 °C for 24 h, respectively. Upon curing, the samples were dried at 80 °C for 6 h. Subsequently, the compressive strength of the samples was tested using a WDW-100 compressive strength machine (Institute of automation of Chinese academy of sciences, China, compressing at a rate of 0.2 kN/min). Finally, all cured samples were ground to powders and the powders of 75–125 μm in diameter were collected for further measurements. The samples were analyzed by XRD and scanning electron microscope (Hitachi S2000, Japan). X-ray powder diffraction patterns were recorded on a D/Max-IIIA machine (Rigaku Industrial Corporation, Japan) using Cu Kα Radiation (40 kV, 30 mA) with a scanning rate of 2°/min from 5° to 70° (2θ).

2.3. Static adsorption measurements

Sample powder 0.1 g was added to a 50 ml solution of 0.002 mol L^{-1} $Sr(NO_3)_2$ and CsCl, respectively, and then immersed completely in a glass bottle for 7 days. All sample bottles were vibrated by an HY-2 vibratory machine (frequency: 40 cyc.per min.) for 3 h per day. After 7 days treatment, the mixtures were separated centrifugally. The Sr and Cs ions in the solutions were determined by using an AA-7003 absorption atomic spectrophotometer with an air-acetylene flame. The absorption rate is calculated via the following function:

$$\eta = \frac{C_0 - C_t}{C_0} \times 100\%$$

where C_0, Sr or Cs is the ion concentration in the original solution, mmol ml^{-1}; C_t, Sr or Cs is the concentration in the solution treated for t time, mmol ml^{-1};

Table 2
The chemical composition of simulated high-alkaline waste (wt.%).

Component	Composition	Component	Composition
Na_2O	90.62	NO_3^-	31.30
Al_2O_3	4.71	SO_4^{2-}	1.72
SrO	0.51	Cl^-	0.29
Cs_2O	0.88	OH^-	63.17
Cr_2O_3	0.76	CO_3^{2-}	3.51
Fe_2O_3	2.52	–	–

Table 3
The molar ratio of cations in AMSHC samples.

Sample	Na:Ca:Al:Si
AMSHC00-00-90,120,180	1:0:1:1
AMSHC10-00-90,120,180	1:0.12:1.03:1.09
AMSHC20-00-90,120,180	1:0.26:1.08:1.19
AMSHC30-00-90,120,180	1:0.44:1.15:1.33
AMSHC40-00-90,120,180	1:0.68:1.24:1.51
AMSHC50-00-90,120,180	1:1.02:1.36:1.77
AMSHC20-20-90,120,180	1:0.32:1.04:1.15
AMSHC20-30-90,120,180	1:0.32:1.03:1.14
AMSHC20-40-90,120,180	1:0.30:0.98:1.08
AMSHC20-50-90,120,180	1:0.29:0.92:1.03

2.4. Product consistency test (PCT)

Referencing to PCT-A (ASTM C1285-97), a modified product consistency test was carried out for leaching tests of ions. In order to interpret the degree of conversion of metakaolin, slag and sodium hydroxide solution to alumino-silicates crystalline phases, the release rates of ions during the PCT for 24 h rather than 7 days were used to determine the effects of curing temperature on the reaction rates. The procedure of the PCT can be described as follows: a suspension of 1 g sample powder in 10 ml deionized water was put in a sealed Teflon vessel, and cured at 90 °C for 24 h. Upon treatment, the vessel was air-cooled and then reweighed. The mixtures were separated centrifugally, and the ion content in the solution was determined by an AA-7003 absorption atomic spectrophotometer and a TH-900 ion chromatograph (Wuhan Tianheng Automation Meter Co. Ltd., China), respectively.

3. Results and discussion

3.1. Mineral phases and properties of AMSHC matrixes

3.1.1. XRD and SEM analyses

Fig. 1 shows XRD patterns of the AMSHC samples cured at 90 °C and 180 °C, respectively. Results reveal that NaA zeolite, sodalite and tobermorite are major mineral phases of the AMSHC matrixes, and the intensity of the diffraction spectra of sodalite and tobermorite are getting stronger with adding slag and elevating temperature. Under such conditions, an addition of slag from 0 to 50 wt.%, Ca/(Si + Al) molar ratio is varied from 0 to 0.32, conversely, Na/(Si + Al) molar ratio is varied from 0.50 to 0.32. Because of the respective change of oxide components content in the system Na_2O–CaO–Al_2O_3–SiO_2, the initial atomic ratio (Na: Ca: Al: Si = 1:0:1:1) was changed accordingly. Naturally, a series of mineral phase's transformation may be caused in AMSHC matrixes. Of these phases, NaA zeolite is easier to be formed from a mixture of metakaolin by alkali activation. And once an available thermo-

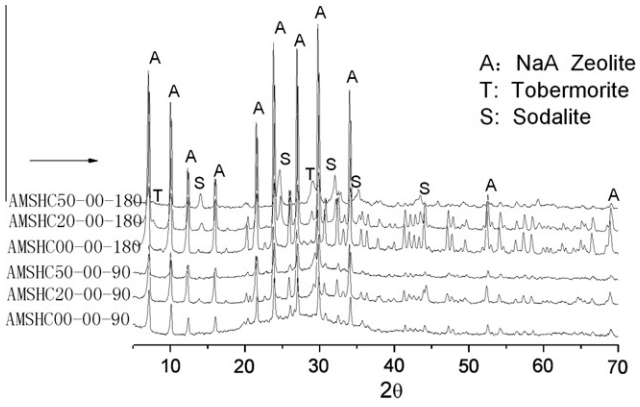

Fig. 1. XRD patterns of AMSHC matrixes cured at 90 °C and 180 °C, respectively.

dynamics circumstance [15–19] is supplied, it may transform to sodalite spontaneously. The Ostwald's law of successive transformation demonstrated the mechanism that the less thermodynamically stable phase of sodium alumino-silicate may be kinetically disposed and precipitated firstly, and then transforms to the more stable phase under the conditions. Tobermorite, a semi-crystal phase of calcium silicate hydrate (C–S–H) gel, may be observed usually in the accelerated curing products of C–S–H [19], whose formation is relative to the use of a slag in this work.

A series of scanning electron microscope (SEM) images of AMSHC are used to check their morphologies. Fig. 2 shows the mineral phase appearance of several AMSHC matrixes. The mineral phase of NaA zeolite appears an intact cubic-like shape comparatively in AMSHC00-00-180, and a petal-like appearance of tobermorite is present in AMSHC20-00-180. Even with the same chemical proportion, the crystallization of NaA zeolite in AMSHC00-00-180 cured hydrothermally at 180 °C is better than that in AMSHC00-00-90 cured hydrothermally at 90 °C. The results reveal that higher curing temperature may accelerate the chemical transformation and cause a rapid crystal growth.

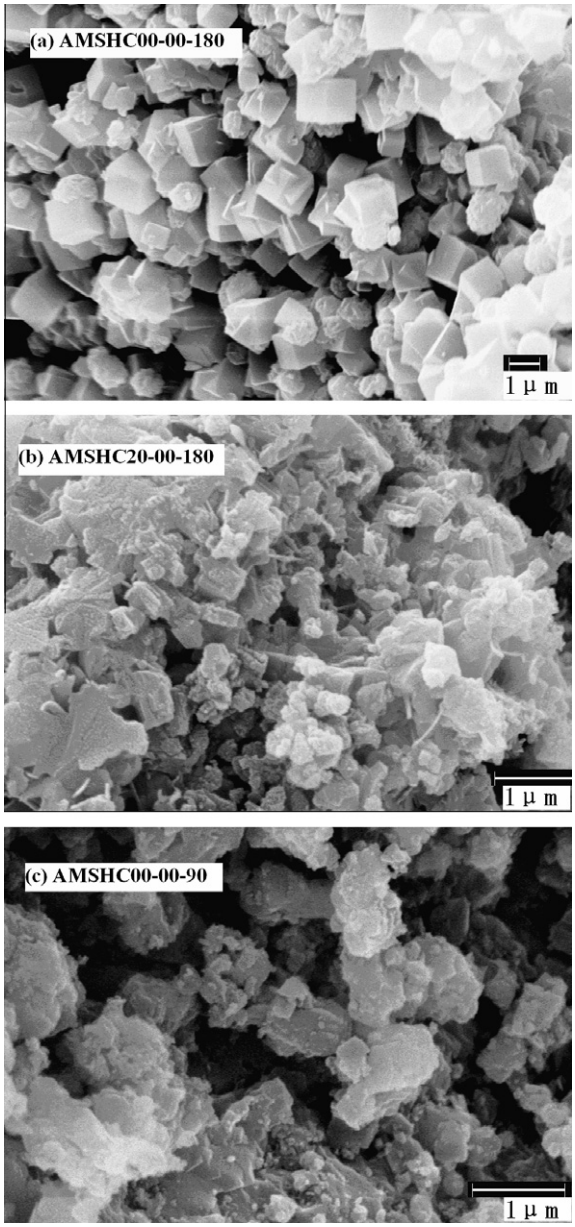

Fig. 2. SEM images of AMSHC matrixes (a–c).

3.1.2. Adsorption capacity to Sr, Cs

Fig. 3 exhibits a correlation of the absorption ratio (η) of Sr and Cs ions to the dosage of slag. One may see that the value of η dramatically decreases with the increase of the addition of slag and the elevated curing temperature. It also indicates that the adsorp-

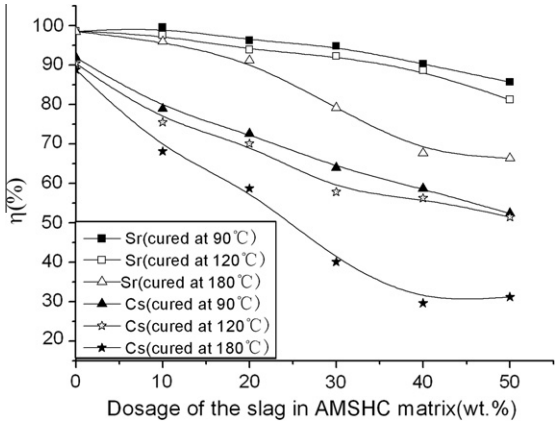

Fig. 3. The curves of absorption rate of Sr^{2+} and Cs^{+}.

Table 4
The pore characterization of the AMSHC matrix cured at 180 °C.

Specimen	Pore size (nm)	Pore distribution (%)	Total pore volume (ml $g^{-1} \times 10^{-3}$)
AMSHC00-00-180	75.7–15.27	81.53	17.70
	15.27–8.72	9.21	
	<8.72	8.77	
AMSHC10-00-180	80.1–15.25	71.33	48.77
	15.25–8.70	13.64	
	<8.70	13.70	
AMSHC20-00-180	79.8–15.20	75.46	51.62
	15.20–8.75	12.92	
	<8.75	10.62	
AMSHC30-00-180	88.9–15.10	84.67	84.67
	15.10–8.77	8.12	
	<8.77	6.13	
AMSHC50-00-180	75.8–15.15	93.23	108.05
	15.15–8.78	4.23	
	<8.78	2.46	

Table 5
The compressive strengths of AMSHC matrixes.

Sample	Average compressive strength (MPa)	Dosage of NaOH (wt.%)
AMSHC00-00-90	3.00	26.34
AMSHC10-00-90	5.50	24.34
AMSHC20-00-90	22.00	22.06
AMSHC30-00-90	22.25	19.70
AMSHC40-00-90	22.50	17.24
AMSHC50-00-90	28.00	14.53
AMSHC00-00-120	5.25	26.34
AMSHC10-00-120	6.75	24.34
AMSHC20-00-120	24.25	22.06
AMSHC30-00-120	25.75	19.70
AMSHC40-00-120	26.75	17.24
AMSHC50-00-120	31.50	14.53
AMSHC00-00-180	8.25	26.34
AMSHC10-00-180	14.28	24.34
AMSHC20-00-180	25.00	22.06
AMSHC30-00-180	25.00	19.70
AMSHC40-00-180	28.00	17.24
AMSHC50-00-180	40.08	14.53

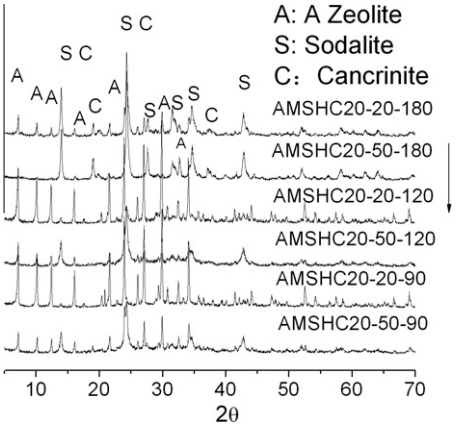

Fig. 4. XRD patterns of AMSHC simulated high-alkaline waste forms.

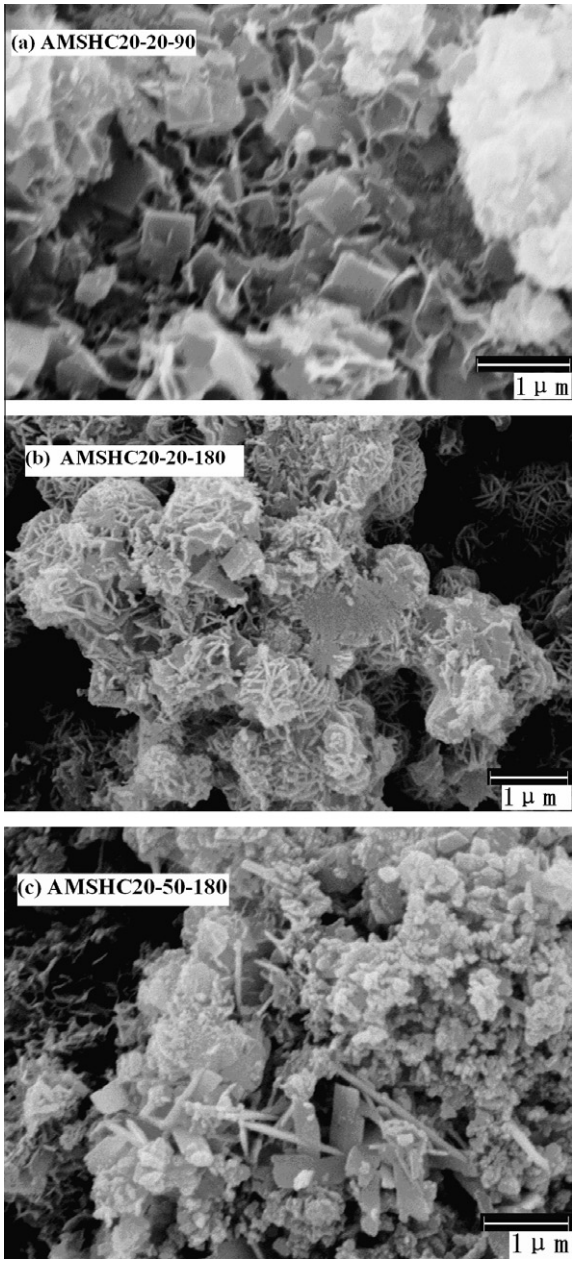

Fig. 5. SEM image of AMSHC simulated high-alkaline waste forms (a–c).

tion capacity of NaA zeolite to Sr and Cs ions is much more improved than the other mineral phases of an AMSHC matrix. As a three dimensional zeolite framework, NaA zeolite is constructed by some units called "cages". Each cage is built by silicon and aluminum tetrahedral structures and it make the cages connected to each other via a double four-ring. Such structure allows hosting ions and molecules by lattice positions, channels and voids. Although sodalities possess a zeolite structure, the cage connection is closed more tightly than a NaA zeolite, whose structure characteristics may be disadvantage to entry for the cations, and consequently leads to a negative influence on the adsorption capacity of ASMHC matrixes. In addition, the pore characterization of ASMHC matrixes cured at 180 °C is listed in Table 4, it indicates that most of pore is centralized on a size range of 15–80 nm and the total pore volume is increasing with increasing dosage of a slag in the composition. Therefore, the incorporation of excessive slag to ASMHC urges the occurrence of amounts of large size pores and in turn is unfavorable to ether adsorption capacity to cations or immobilization of radioactive waste.

3.1.3. Compressive strength

Although the incorporation of slag to ASMHC is disadvantage to adsorption capacity, the results of the compressive strength tests, as listed in Table 5, indicate that the compressive strength of AMSHC matrixes may be improved effectively by the addition of slag and the elevated curing temperature. Slag, as a starting material, is used widely in concretes and various building materials due to its potential to enhance mechanical properties. So, it may also improve the compressive strength for AMSHC matrixes. Furthermore, the elevated curing temperature may accelerate the hydration reaction of AMSHC matrixes, and the compressive strength may be thus improved correspondingly. On the other hand, according to Jaarsveld's research [20], the connection strength of "–Si–O–Si–" bond is stronger than "–Al–O–Al–" bond in alumino-silicate frameworks. consequently, when the reduce of Al/Si molar ratio and a corresponding increase of the amount of "–Si–O–Si–" bonds occurs, the mechanical properties of the hydrated products may be improved. In our study, Al/Si molar ratio is varied from 1 to 0.77 while the addition of slag increase from 0 to 50 wt.%. The results of the mechanical properties of AMSHC matrix are in coincidence with the structure-forming mechanism.

3.2. Mineral phases and properties of AMSHC simulated highly-alkaline waste forms

3.2.1. XRD and SEM results

From the above discussion, we can conclude that addition of a slag cannot only improve the compressive strength, but also decrease the adsorption capacity of AMSHC matrixes. In order to obtain better immobilization and mechanical properties, AMSHC20-

Table 6
The PCT leaching fraction of ions (wt.%).

Sample	NO_3^-	Cl^-	SO_4^{2-}	Sr^{2+}	Cs^+	Na^+	Cr^{3+}	Fe^{3+}
AMSHC20-20-90	37.00	86.69	87.26	8.75	9.24	36.92	0.34	0.06
AMSHC20-30-90	24.40	87.66	79.43	7.73	7.90	37.32	0.34	0.06
AMSHC20-40-90	18.87	59.51	52.48	2.92	7.31	35.56	0.25	0.06
AMSHC20-50-90	9.58	27.92	45.30	3.51	5.41	32.16	1.37	0.05
AMSHC20-20-120	18.93	63.64	54.58	5.19	8.41	36.92	0.11	0.04
AMSHC20-30-120	4.72	25.11	33.48	4.80	5.51	31.03	0.18	0.02
AMSHC20-40-120	5.71	24.32	26.24	4.19	4.58	32.88	0.16	0.02
AMSHC20-50-120	2.21	10.36	37.24	2.80	4.27	27.24	0.32	0.02
AMSHC20-20-180	1.36	27.60	40.84	2.17	2.50	17.49	1.49	0.05
AMSHC20-30-180	1.74	19.38	27.89	1.87	1.90	20.82	1.26	0.19
AMSHC20-40-180	2.57	13.88	32.93	0.92	1.48	15.68	2.31	0.04
AMSHC20-50-180	2.80	10.54	31.66	0.60	0.85	17.40	3.81	0.05

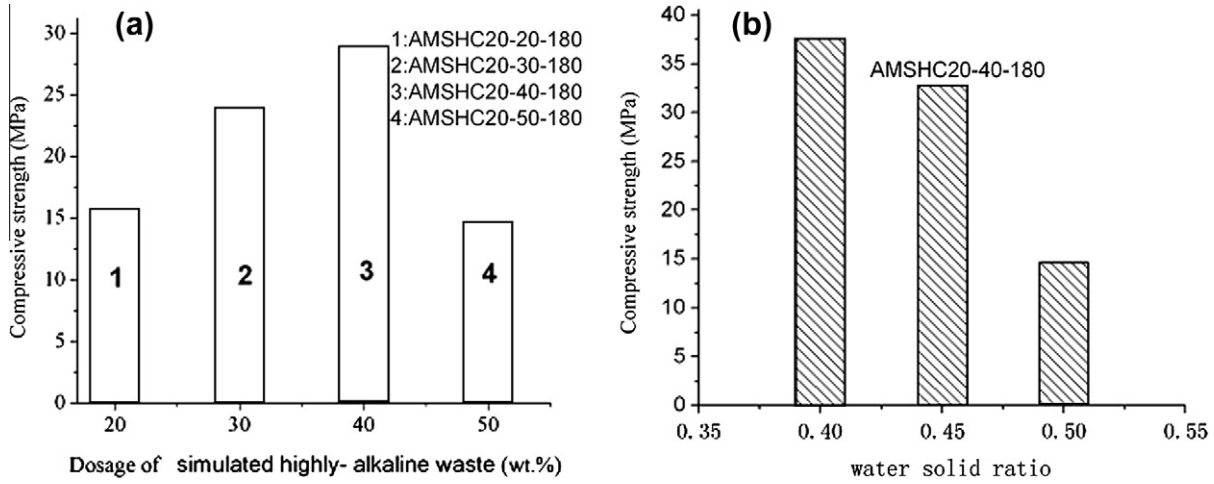

Fig. 6. The compressive strength of several AMSHC simulated high-alkaline waste forms.

00-*Z* (*Z*: curing temperature) samples were chosen for immobilization property evaluation.

Fig. 4 shows that NaA zeolite, sodalite and cancrinite are the major mineral phases of AMSHC simulated highly-alkaline waste forms, and the diffraction spectra peaks of sodalite and cancrinite become higher gradually with adding simulated highly-alkaline waste and elevating curing temperature.

Fig. 5 shows the images of several mineral phases of AMSHC simulated highly-alkaline waste forms, i.e., a cubic NaA zeolite in AMSHC20-20-90, a rounded shape of sodalite in AMSHC20-20-180 and a column-like shape of cancrinite in AMSHC20-50-180. We can see from these images that the coexistence of several mineral phases reveal an existence of a correlation of phase transformation in AMSHC. Some researches [21–23] reported that cancrinite can be formed from NaA zeolite and sodalite under some conditions such as in a hydrothermal circumstance and in inorganic slat media, and the sequence of the transformation of the mineral phases would be as follows, Alumino-silicate species → Amorphous phase → Zeolite → Sodalite → Cancrinite. The experiments satisfactorily supply some inherent conditions such as alkaline media and salt molecules, and exterior conditions such as hydrothermal conditions for the formation of these phases for the high performance hydroceramics.

3.2.2. Immobilization properties and compressive strength of AMSHC waste forms

Table 6 gives the results of PCT. It reveals that the leaching percent fraction of all ions except for Fe and Cr are almost decreasing with the addition of the wastes and an elevated curing temperature. The decrease of ions releases is correlative to the evolution of major mineral phases in the ASMHC waste forms. Actually, during the chemical and physical processing of AMSHC simulated highly-alkaline waste forms, Na, Sr and Cs ions are ineluctably introduced, and combined with aluminum and silicon to form zeolite structures. The formation of the new bonds for zeolite also involves a combination of various slat molecules and the structural rearrangement of metakaolin to achieve a thermodynamic stability. With the stability of the structures, most of the ions and molecules can be hosted tightly to the networks of major mineral phase in AMSHC. Furthermore, according to a literature [24], low Cs and Sr releases can be achieved by the occupation of Cs and Sr ions in the framework position of alumino-silicate polymers with high degree of polymerization, which is achieved by lower Si/Al molar ratio (a optimum Si/Al molar ratio is 2). In present work, the design of the Si/Al molar ratio closed to 1 is to expect to develop a zeolite structure [25] so as to achieve higher degree of polymerization and consequently supply more framework position for the occupation of Cs and Sr ions. On the basis of higher degree of polymerization, the release of Cs and Sr ions can be further decreased with the crystal growth of zeolite minerals under an elevated curing temperature.

Fig. 6 shows that the compressive strength of the simulated highly-alkaline waste forms are increasing with the increase of the addition of the wastes and the curing temperature and the decrease of the ratio of water to solid, but the result about AMSHC20-50-180 did not obey the rule. Presumably, It is because that water to solid ratio for AMSHC20-50-180 is actually 0.50 (for keeping a 50% addition of waste) but higher than 0.45 in other samples.

4. Conclusions

The present work has investigated the mineral phases and the mechanical and immobilization properties of AKHSC. It showed that the mechanical and immobilization properties are determined mainly by the chemical composition of the AKHSC and the curing conditions. Adding a slag to AMSHC matrixes can enhance the compressive strength, but also reduce its adsorption capacity to Sr and Cs ions because of the decrease of a relative content of zeolite phases. In addition, the AMSHC simulated highly-alkaline waste forms exhibit a series of phase transformation with adding simulated highly-alkaline waste liquid and elevating temperature. Due to the difference of the mineral phase in AMSHC, it also determined finally the immobilization and mechanical properties of AMSHC.

Acknowledgments

The authors would like to give thank to the Institute of Nuclear Physics and Chemistry, China Academy of Engineering Physics and School of materials science and Engineering, Southwest University of Science and Technology of China for providing facilities to carry out the work.

Reference

[1] I.W. Donald, B.L. Metcalfe, R.N.J. Taylor, J. Mater. Sci. 32 (1997) 5851.
[2] W.E. Lee, M.I. Ojovan, M.C. Stennett, N.C. Hyatt, Adv. Appl. Ceram. 105 (2006) 3.
[3] C.M. Janzen, K.G. Brown, J.B. Pickett, Int. J. Appl. Glass Sci. 1 (2010) 38.
[4] E.R. Maddrell, J. Am. Ceram. Soc. 84 (2001) 1187.
[5] H.J. Matake, I.L.F. Ray, B.W. Seatonberry, H. Thiele, C. Trisoglio, C.T. Walker, et al., J. Am. Ceram. Soc. 73 (1990) 370.

[6] R.C. Ewing, W.J. Weber, J. Lian, J. Appl. Phys. 95 (2004) 5949.
[7] A.E. Ringwood, S.E. Keesson, N.G. Ware, W. Hibberson, A. Major. Nat. 278 (1979) 219.
[8] W.L. Gong, W. Lutze, R.C. Ewing, J. Nucl. Mater. 278 (2000) 73.
[9] P. Losieau, D. Caurant, O. Majerus, N. Baffier, L. Mazerolles, C. Fillet, Phys. Chem. Glass. 43 (2002) 195.
[10] D.D. Siemer, Mater. Res. Innov. 6 (2002) 96–104.
[11] Yun Bao, Stephen Kwan, Darryl D. Siemer, J. Mater. Sci. 2 (2004) 481–488.
[12] Mary Lou Dunizk Gougar, Barry E Scheetz, D.D. Siemer, Radio Waste Manage. Disposal 125 (1999) 93–103.
[13] M.I. Ojovan, O.G. Batyukhnova, In: WM'07 Conference, Tucson, AZ, 2007.
[14] M.I. Ojovan, W.E. Lee, An Introduction to Nuclear Waste Immobilisation, Elsevier Science, Amsterdam, 2005. pp. 109–113.
[15] B. Subotic, D. Skritic, I. Smit, L. Sekovanic, J. Cryst. Growth 50 (1980) 498.
[16] M. Tassopoulos, R.W. Thompson, Zeolites 7 (1987) 243.
[17] Lin. Dechang, Micropor. Mesopor. Mater. 70 (2004) 63.
[18] A. Fernandez Jimenez, M. Monzo, M. Vicent, Micropor. Mesopor. Mater. 108 (2008) 41.
[19] Michael Grutzeck, Stephen Kwan, Maria DiCola, Cem. Concr. Res. 34 (2004) 949.
[20] J.G.S. van Jaarsveld, J.S.J. van Deventer, Cem. Concr. Res. 29 (1999) 1189.
[21] Mark.C. Barnes, Jonas. Addai-Mensah, Andrea.R. Gerson, Micropor. Mesopor. Mater. 31 (1999) 287.
[22] Y.J. Deng, J.B. Harsh, M. Flury, J.S. Young, J.S. Boyle, Appl. Geochem. 21 (2006) 1392.
[23] Mark C. Barnes, Jonas Addai-Mensah, Andrea R. Gerson, Colloids Surf. A 157 (1999) 101.
[24] Z. Aly, E.R. Vance, D.S. Perera, J.V. Hanna, C.S. Griffith, J. Davis, et al., J. Nucl. Mater. 378 (2008) 172.
[25] Matthew Rowles, Brian O'Connor, J. Mater. Chem. 13 (2003) 1161.